

RIC-3 phosphorylation enables dual regulation of excitation and inhibition of *Caenorhabditis elegans* muscle

Gracia Safdie^a, Jana F. Liewald^b, Sarah Kagan^a, Emil Battat^a, Alexander Gottschalk^b, and Millet Treinin^{a,*}

^aDepartment of Medical Neurobiology, Institute for Medical Research Israel-Canada, Hebrew University–Hadassah Medical School, Jerusalem 91120, Israel; ^bBuchmann Institute for Molecular Life Sciences and Institute of Biochemistry, Goethe-University, D-60438 Frankfurt, Germany

ABSTRACT Brain function depends on a delicate balance between excitation and inhibition. Similarly, *Caenorhabditis elegans* motor system function depends on a precise balance between excitation and inhibition, as *C. elegans* muscles receive both inhibitory, GABAergic and excitatory, cholinergic inputs from motor neurons. Here we show that phosphorylation of the ER-resident chaperone of nicotinic acetylcholine receptors, RIC-3, leads to increased muscle excitability. RIC-3 phosphorylation at Ser-164 depends on opposing functions of the phosphatase calcineurin (TAX-6), and of the casein kinase II homologue KIN-10. Effects of calcineurin down-regulation and of phosphorylated RIC-3 on muscle excitability are mediated by GABA_A receptor inhibition. Thus RIC-3 phosphorylation enables effects of this chaperone on GABA_A receptors in addition to nAChRs. This dual effect provides coordinated regulation of excitation and inhibition and enables fine-tuning of the excitation–inhibition balance. Moreover, regulation of inhibitory GABA_A signaling by calcineurin, a calcium- and calmodulin-dependent phosphatase, enables homeostatic balancing of excitation and inhibition.

Monitoring Editor

Jonathan Chernoff
Fox Chase Cancer Center

Received: May 3, 2016

Revised: Jul 5, 2016

Accepted: Jul 26, 2016

INTRODUCTION

A balance between excitation and inhibition is required for normal function of the nervous system. Excitation–inhibition (E-I) imbalance leads to epilepsy, is associated with autism spectrum disorders, and has also been implicated in Alzheimer's disease (Eichler and Meier, 2008; Lei *et al.*, 2016). Thus understanding mechanisms regulating E-I balance is of great importance. The *Caenorhabditis elegans* body-wall muscle cells provide an experimentally tractable and well-characterized system in which to study mechanisms regulating E-I balance because they receive innervation from excitatory, cholinergic

motor neurons, as well as from inhibitory, GABAergic motor neurons. In body-wall muscle, acetylcholine (ACh) activates two subtypes of nicotinic acetylcholine receptor (nAChR)—levamisole-sensitive nAChR (L-AChR) and nicotine-sensitive nAChR (ACR-16)—whereas GABA activates the GABA_A receptor (UNC-49; Richmond and Jorgensen, 1999).

Levamisole, an agonist of L-AChR, provides a powerful tool for identifying and characterizing genes participating in synaptic transmission at the neuromuscular junction. Screens for levamisole resistance identified subunits of L-AChR and proteins needed for maturation and normal functioning of L-AChR (Lewis *et al.*, 1980a,b; Martin *et al.*, 2012). In addition, hypersensitivity to levamisole identified both presynaptic and postsynaptic components needed for regulating synaptic transmission, including multiple kinases and a phosphatase (TAX-6, a calcineurin A homologue, Gottschalk *et al.*, 2005; Vashlishan *et al.*, 2008; Jospin *et al.*, 2009). The targets of these kinases or of TAX-6 in body-wall muscles are, however, unknown.

RIC-3 is a conserved endoplasmic reticulum (ER)-resident chaperone known to affect maturation of multiple nAChRs (Halevi *et al.*, 2002, 2003). Loss of RIC-3 function leads to levamisole resistance and reduces the functional expression of both body-wall

This article was published online ahead of print in MBoc in Press (<http://www.molbiolcell.org/cgi/doi/10.1091/mboc.E16-05-0265>) on August 3, 2016.

*Address correspondence to: Millet Treinin (millet.treinin@mail.huji.ac.il).

Abbreviations used: ACh, acetylcholine; CaM, calmodulin; dsRNA, double-stranded RNA; E-I, excitation–inhibition; ER, endoplasmic reticulum; GFP, green fluorescent protein; lf, loss-of-function; L-AChR, levamisole-sensitive acetylcholine receptor; nAChR, nicotinic acetylcholine receptor; WT, wild type; YFP, yellow fluorescent protein.

© 2016 Safdie *et al.* This article is distributed by The American Society for Cell Biology under license from the author(s). Two months after publication it is available to the public under an Attribution–Noncommercial–Share Alike 3.0 Unported Creative Commons License (<http://creativecommons.org/licenses/by-nc-sa/3.0>).

"ASCB[®]," "The American Society for Cell Biology[®]," and "Molecular Biology of the Cell[®]" are registered trademarks of The American Society for Cell Biology.

MPKTERRRDRDRDRDRERRRNRKRDDSYDDY
DEEGGI SGWKLGLVFGVIVVCFAMLYPTLFH
PMLMGFLGRSPSPSPSINQQRPP IHPAMGGG
SGQRHPGGGADVHPAMRMAQAQAE SQSGGSK
GMFTWMLPVYTI GVVLFLLYTLFKSKGKSK
RKRKNYFD SEDDDDE SESE TKYGGKFGKKKL
EC LQKRLRETE SAMSKILEQLE SVQAGANPV
DLDAADRSEQLEEDPSVKEAVGLTETNEQY
IKDLEVALKEFQSL SKEYDKAKMKLKRKDS
SSEDEEEDDEEENSSELSE IEEEEEEVKPVKK
SKSSSQSVGKRKRNRPKSTSEEEDEGEEESRK
VAEDAE EEGIDIDSE IREHAEKEKKDKNVR
RRPKKT

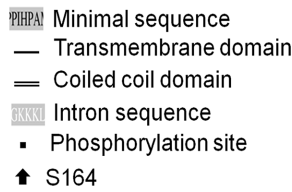


FIGURE 1: Sequence of the *C. elegans* RIC-3. Highlighted in gray is the sequence of the minimal *ric-3*-rescuing fragment. White letters on gray indicate sequence of the alternatively spliced intron missing in the minimal fragment. The transmembrane domains are single underlined, and the coiled-coil domains are double underlined. Residues shown to be phosphorylated by Zielinska *et al.* (2009) are italicized and indicated by dots. Arrow, Ser-164.

muscle nAChRs but not of the GABA_A receptor expressed in these muscles (Halevi *et al.*, 2002); across evolution, RIC-3 regulates functional expression of multiple divergent nAChRs and their close relatives, 5HT3 receptors, but shows no effects on other, more distant members of the Cys-loop family of ligand-gated ion channels (Halevi *et al.*, 2002, 2003; Cheng *et al.*, 2005; Lansdell *et al.*, 2005). The key role of RIC-3 in maturation of multiple diverse nAChRs suggested that its regulation enables modulation of cholinergic signaling. Indeed, regulation of RIC-3 quantity via interaction with the CUL-3 adaptor BATH-42 was shown to regulate L-AChR activity in *C. elegans* vulval muscles (Shteingauz *et al.*, 2009). Moreover, a phosphoproteomic screen showed that in *C. elegans*, RIC-3 is phosphorylated at multiple sites in vivo (Zielinska *et al.*, 2009).

Here we examine the function of RIC-3 phosphorylation to show that phosphorylation of RIC-3 Ser-164 enhances *C. elegans* body-wall muscle excitability. We identify TAX-6 (calcineurin A homologue) and KIN-10 (casein kinase II homologue) as likely to function reciprocally in controlling phosphorylation of RIC-3 at Ser-164. Furthermore, we show that effects of TAX-6 and of RIC-3 Ser-164 phosphorylation are mediated by reduced functional expression of the inhibitory GABA_A receptor rather than by enhanced nAChR functional expression. Thus we identify a new target for RIC-3 and a novel mechanism for coordinated regulation of excitatory and inhibitory inputs.

RESULTS

Phosphorylation of RIC-3 Ser-164 enables enhanced muscle excitability

To identify targets of signaling pathways regulating body-wall muscle excitability, we examined a database of *C. elegans* phosphorylation sites identified by phosphoproteomics (www.phosida.com; Zielinska *et al.*, 2009) for phosphorylation of muscle-expressed receptor subunits and proteins needed for maturation of these receptors (these proteins and references for their function in *C. elegans* body-wall muscle are listed in Supplemental Table S1). This analysis identifies RIC-3 as a strong candidate for regulation by phosphorylation, as five of its residues are phosphorylated in vivo, whereas for the other proteins examined, no or fewer phosphorylated sites could be identified (except for NLG-1; Supplemental Table S1). RIC-3 is an evolutionarily conserved chaperone of nAChRs shown to

affect surface expression and activity of both body-wall muscle nAChRs (Halevi *et al.*, 2002). Thus phosphorylation/dephosphorylation of RIC-3 may affect levamisole responsiveness via regulation of L-AChR functional expression.

To examine the role of RIC-3 phosphorylation in controlling muscle excitability, we generated mutations in RIC-3 phosphorylation sites, focusing on RIC-3 Ser-164, the only phosphorylation site in the minimal rescuing RIC-3 fragment (Figure 1 and *Materials and Methods*). To eliminate confounding effects due to the phosphorylation state of other RIC-3 residues, we generated Ser-164 mutations within this minimal RIC-3 fragment, a fragment previously shown to fully rescue functional expression of body-wall muscle nAChRs (Biala *et al.*, 2009). Expression of RIC-3 minimal and two Ser-164 mutants—S164A, eliminating phosphorylation,

and S164E, mimicking phosphorylation—under a *ric-3(md1181)* loss-of-function background rescued the levamisole resistance of *ric-3(md1181)* animals, demonstrating that all three proteins are functional. Moreover, the S164E mutation led to significant levamisole hypersensitivity within 15 min of exposure (Figure 2A), whereas levamisole responsiveness of animals expressing the S164A mutation was similar to the responsiveness of animals expressing wild-type RIC-3 (Figure 2A).

RIC-3 affects nAChR activity in motor neurons and regulates neurotransmitter release and E-I balance via regulation of this nAChR (Jospin *et al.*, 2009). Thus levamisole hypersensitivity of the S164E mutant could be a result of perturbation of E-I balance due to neuronal expression of this mutant. To examine whether effects of RIC-3 S164E depend on muscle expression of this mutant protein, we compared levamisole responsiveness of animals expressing the RIC-3 S164E mutant protein under a muscle-specific promoter to control animals expressing the wild-type protein under the same promoter. The muscle-expressed wild-type and S164E transgenes were injected into a wild-type background to avoid masking effects due to reduced GABA release by inhibitory motor neurons whose activity depends on the ACR-12 nAChR, which is likely to require RIC-3 function for its expression (Petrasch *et al.*, 2013). Results of this analysis (Figure 2B) showed that muscle-expressed S164E enhances levamisole sensitivity relative to the wild-type protein expressed from the same promoter. Therefore muscle expression of the S164E mutation is sufficient to confer levamisole hypersensitivity to body-wall muscles (Figure 2B). Moreover, effects of the S164E mutation are dominant over wild-type RIC-3. Note that levamisole sensitivities in Figure 2B are lower than in Figure 2A. Indeed, kinetics of the response and overall sensitivity to levamisole in our experimental setup depend on several variables, including temperature and transgene. Thus comparisons between strains or treatments were done within the same experiment (day) and using appropriate controls; in Figure 2B, the same RIC-3 construct differed by a single amino acid.

Previously we showed that mechanisms regulating RIC-3 quantity affect muscle excitability (Shteingauz *et al.*, 2009). To examine whether the S164E mutation affects RIC-3 quantity, we quantified the fluorescence intensity of green fluorescent protein (GFP)-tagged versions of wild-type and S164E RIC-3 proteins. To better observe muscle distribution of these proteins, we used the muscle-specific

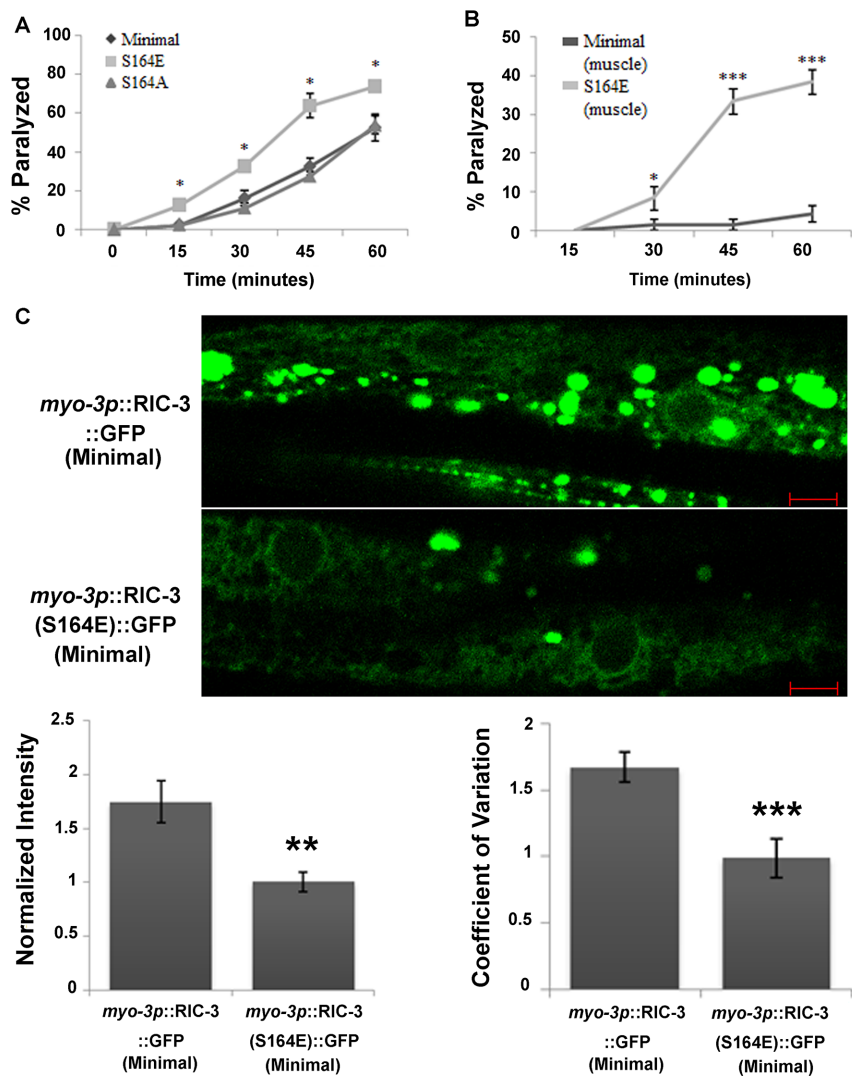


FIGURE 2: Phosphorylation of Ser-164 enhances muscle excitability and reduces RIC-3 quantity. (A) Levamisole sensitivity of animals expressing the minimal RIC-3 fragment (diamonds) or the same fragment having the S164A mutation (triangles) or the S164E mutation (squares), all under a *ric-3* promoter in a *ric-3(md1181)* (loss-of-function) background. Percentage of animals paralyzed at different time points after being placed on plates containing levamisole (0.2 mM). Significance is relative to minimal RIC-3-expressing animals at the same time point; eight plates and four independent experiments. (B) Levamisole sensitivity of animals expressing minimal RIC-3 (dark gray) or minimal RIC-3 S164E (light gray) expressed from a muscle-specific promoter, *myo-3p*, and in a wild-type background. Percentage of animals paralyzed at different time points, as described in A. Significance is relative to minimal RIC-3-expressing animals at the same time point; six or seven plates and three independent experiments. (C) Quantity and distribution of RIC-3::GFP and RIC-3(S164E)::GFP expressed from a muscle-specific promoter. Top, representative images of GFP-tag fluorescence; scale bar, 5 μ m. Bottom left, average intensity; $n = 12$ or 13 , $N = 2$. GFP intensity is normalized to the average GFP intensity in S164E animals imaged in the same experiment/day. Bottom right, coefficient of variation of fluorescence intensity from the same images. * $p < 0.05$, ** $p < 0.01$, *** $p < 0.001$.

transgenes analyzed in Figure 2B having higher expression relative to the same constructs expressed from the *ric-3* promoter. This higher expression may explain the many aggregates seen in control animals, aggregates not seen in antibody staining for the native protein (compare Figures 2C and 3B). Analysis of these images demonstrates significantly reduced expression of the RIC-3 S164E mutant (Figure 2C). Increased RIC-3 expression is associated with increased

of TAX-6 on body-wall muscle L-AChR may be mediated by regulation of RIC-3. Moreover, this reduction is similar to the effects of the RIC-3(S164E) mutation (Figure 2C), suggesting that knockdown of the phosphatase TAX-6 leads to increased Ser-164 phosphorylation and destabilization of RIC-3 in body-wall muscle. To see whether effects of TAX-6 on RIC-3 quantity occur within muscle, we examined RIC-3 quantity in muscle expressing a *tax-6* gain-of-function

RIC-3 aggregation and was suggested to reduce nAChR functional expression by sequestering receptor subunits within non-functional aggregates (Shteingauz et al., 2009). Indeed, we see more aggregates in wild-type muscle than S164E muscle (Figure 2C). To measure the degree of aggregation, we used a measure of distribution homogeneity, the coefficient of variation, as done in Shteingauz et al. (2009). This analysis shows significant reduction of the coefficient of variation in RIC-3 S164E transgenics (Figure 2C). Thus phosphorylation of RIC-3 at Ser-164 is likely to reduce its quantity and increase homogeneity of its distribution due to reduced aggregation. Results presented later, however, suggest that this reduction in quantity and aggregation is not required for effects of Ser-164 phosphorylation on muscle excitability.

RIC-3 Ser-164 is a likely target of TAX-6

TAX-6 was previously shown to reduce levamisole responsiveness of *C. elegans* body-wall muscles. These results were shown using a loss-of-function mutation in *tax-6* or after down-regulation of *tax-6* using double-stranded RNA (dsRNA) feeding in strains sensitized for effects of dsRNA feeding (Gottschalk et al., 2005). Effects of TAX-6 on levamisole responses of body-wall muscles were shown to mostly depend on muscle expression, although some effects were suggested to depend on neuronal expression (Gottschalk et al., 2005). To focus on effects of TAX-6 on levamisole responsiveness within muscles, we used dsRNA feeding in wild-type, nonsensitized animals, as *C. elegans* neurons are refractory to dsRNA-mediated interference with gene expression (Sieburth et al., 2005). Using this method for down-regulation of TAX-6, primarily in muscle, we were able to reproduce previous results (Gottschalk et al., 2005). Specifically, we showed that TAX-6 knockdown, like RIC-3 S164E expression, leads to levamisole hypersensitivity (Figure 3A).

To examine whether TAX-6 is likely to target RIC-3, we looked at RIC-3 protein after TAX-6 knockdown using immunohistochemistry. This analysis showed that TAX-6 knockdown leads to a significantly reduced quantity of RIC-3 in muscle (reduction to 40% of control animals; Figure 3B). Thus RIC-3 quantity is regulated by TAX-6, and effects

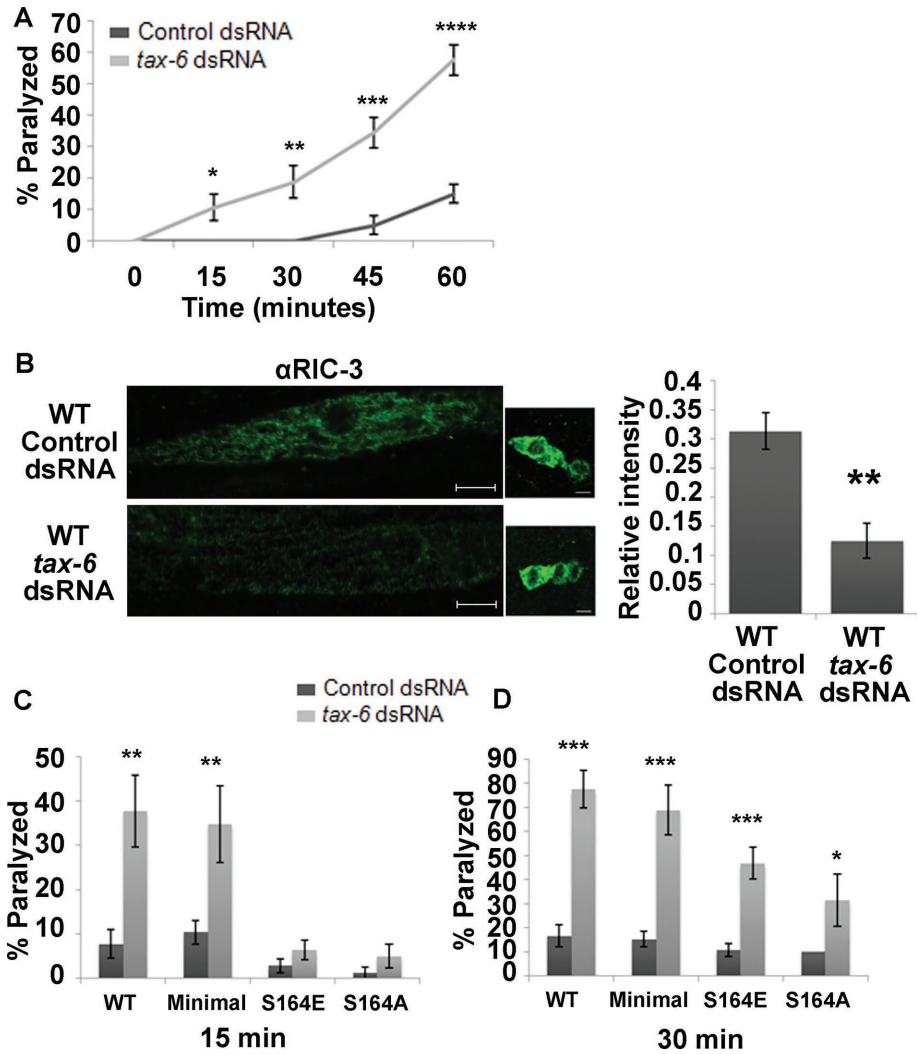


FIGURE 3: TAX-6 knockdown enhances muscle excitability and reduces RIC-3 quantity. (A) Levamisole sensitivity of wild-type animals fed with empty vector– (control; dark gray) or *tax-6* dsRNA–expressing (light gray) bacteria. Percentage of animals paralyzed at different time points after being placed on plates containing levamisole (0.2 mM). Significance is relative to animals fed with control dsRNA at the same time point; four plates and two independent experiments. (B) Quantity of RIC-3 as seen using immunohistochemistry in animals fed with control or *tax-6* dsRNA. Left, representative images of muscles and neurons after each treatment; scale bar, 5 μ m. Right, average intensity relative to intensity of neurons from the same animal. two independent stainings and 9–13 animals from each treatment. (C, D) Effects of TAX-6 knockdown are suppressed by Ser164 mutations. Animals expressing full-length, wild-type (WT) RIC-3, minimal RIC-3 (Minimal), minimal RIC-3 S164E (S164E), or minimal RIC-3 S164A (S164A) in a *ric-3(md1181)* background and treated with control (dark gray) or *tax-6* dsRNA–expressing (light gray) bacteria. Percentage of animals paralyzed at 15 min after being placed on levamisole (C; 8–12 plates and four to seven independent experiments each) or 30 min (D; 8–12 plates and four to seven independent experiments each). Significance is relative to the same strain fed with control dsRNA (empty vector) at the same time point. * $p < 0.05$, ** $p < 0.01$, *** $p < 0.001$, **** $p < 0.0001$.

transgene relative to control, *tax-6* loss-of-function mutants not expressing this transgene (Gottschalk *et al.*, 2005). Results of this analysis showed reduced RIC-3 quantity (25.7%) in *tax-6* loss-of-function mutants relative to mutants expressing the TAX-6 gain-of-function mutant in muscles. These results are consistent with TAX-6 functioning within body-wall muscle to control RIC-3 quantity (Supplemental Figure S1).

If RIC-3 Ser-164 is dephosphorylated by TAX-6, we expect that mutation of this site either to alanine (eliminating phosphorylation) or glutamate (mimicking phosphorylation but resistant to the effects

of TAX-6) will reduce the effects of *tax-6* down-regulation by dsRNA. Indeed, both mutations eliminate effects of TAX-6 down-regulation on levamisole responsiveness of body-wall muscles, as seen soon (15 min) after placing the animals on levamisole-containing plates (Figure 3C). At a later time point (30 min), however, effects of TAX-6 are reduced but not eliminated by mutation of Ser-164 (Figure 3D), suggesting that TAX-6 has additional, unknown targets affecting responsiveness to prolonged levamisole exposure. Ser-164, however, is likely to be the only TAX-6 target within RIC-3, as effects of *tax-6* knockdown on levamisole responsiveness of animals expressing full-length RIC-3 (wild type) or minimal RIC-3 are similar (Figure 3, C and D). We note that, unlike results shown in Figure 2A, S164E transgenics in dsRNA-feeding experiments fed with control (empty vector)-expressing bacteria are not hypersensitive to levamisole compared with control transgenics on the same food source (Figure 3, C and D). This difference suggests that extrinsic factors—possibly the bacterial strain used as food in dsRNA-feeding experiments—affect muscle excitability to mask effects of this mutation.

Effects of TAX-6 are mediated by GABA_A receptor inhibition

To better understand the mechanism enabling effects of TAX-6 on levamisole sensitivity, we examined the quantity of synaptic L-AChR using a yellow fluorescent protein (YFP)-tagged knock-in allele of UNC-63, a subunit of this receptor. This knock-in allele was shown to provide a sensitive assay for synaptic expression of L-AChR (Boulin *et al.*, 2012). Results of this analysis showed no significant change in UNC-63::YFP intensity of TAX-6 dsRNA–treated compared with control synapses (Figure 4A). To validate these results and examine the possibility that TAX-6 affects function but not surface expression of L-AChR, we recorded the electrophysiological responses of whole-cell, patch-clamped body-wall muscles in *tax-6* loss-of-function (*lf*) mutants. This analysis showed no difference in peak current amplitudes elicited by pressure application of levamisole (100 μ M) in *tax-6(lf)* mutants relative to wild-type controls (Figure 4B). Therefore effects of TAX-6 on muscle excitability are not due to enhanced synaptic quantity or levamisole responsiveness of L-AChRs.

Previous analyses showed that reduced inhibitory (GABAergic) inputs to body-wall muscles produced levamisole hypersensitivity (Vashlishan *et al.*, 2008). To examine whether TAX-6 regulates GABA_A activity, we also recorded the responses of *C. elegans* body-wall muscles to GABA (100 μ M) application in *tax-6(lf)* mutants. Note that under the conditions used in our experiments and as previously

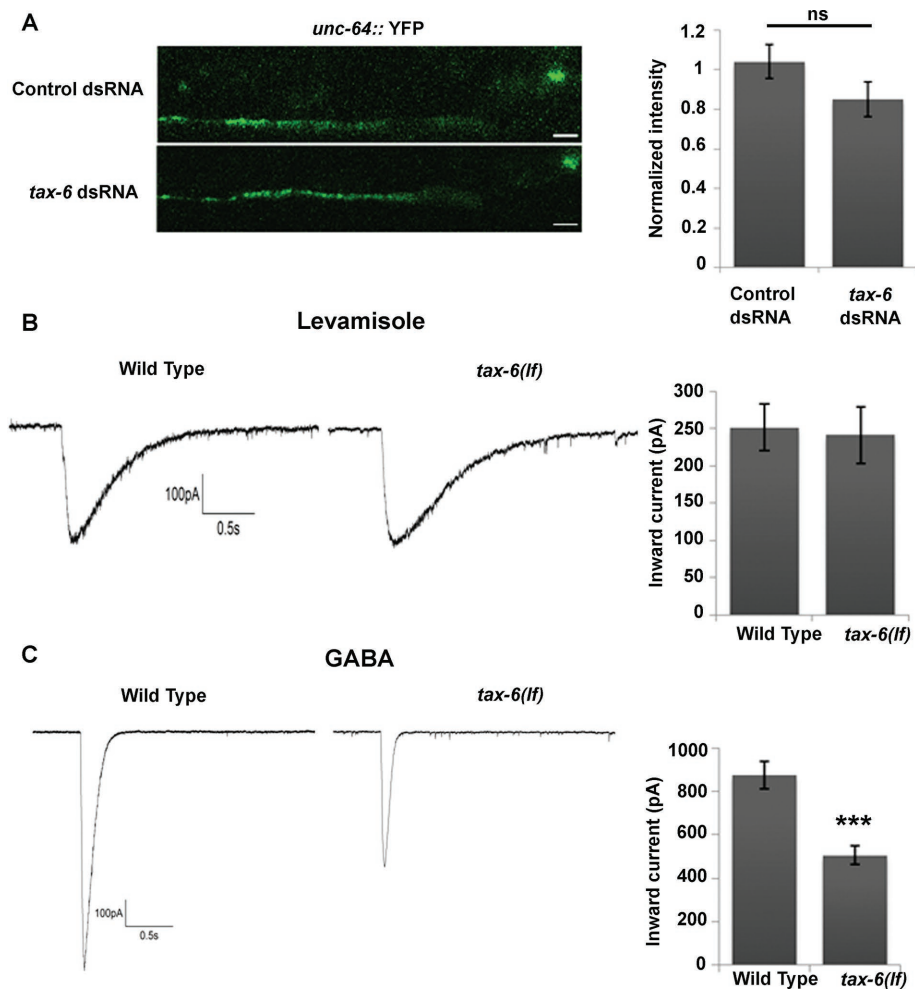


FIGURE 4: Effects of TAX-6 knockdown or loss of function are mediated by GABA_A inhibition. (A) Effects of *tax-6* knockdown on synaptic abundance of UNC-63. YFP intensity in synaptic puncta of animals fed with empty vector (Control) or *tax-6* dsRNA-expressing bacteria. Left, representative images; right, average intensity; $n = 35\text{--}36$ each. YFP intensity is normalized to the average YFP intensity in animals fed with control dsRNA, which were imaged in the same experiment/day. (B, C) Currents recorded from patch-clamped body-wall muscle of wild-type or *tax-6(lf)* animals after application of levamisole (100 μM ; B) or GABA (100 μM ; C). Left, representative traces; right, average peak amplitudes; $n = 7\text{--}9$ each. *** $p < 0.001$.

described, GABA application elicits an outward chloride current, which is unlike the normally inward (inhibitory) currents in intact animals (Richmond and Jorgensen, 1999). Results from this analysis show $\sim 50\%$ reduction in peak current amplitudes in *tax-6(lf)* compared with wild-type animals (Figure 4C). Thus the effects of TAX-6 on muscle excitability are not due to altered excitatory (nAChR) responsiveness but instead can be explained by altered inhibitory (GABA_A receptor) responsiveness.

Effects of phosphorylated RIC-3 Ser-164 are mediated by UNC-49 receptor inhibition

Results in Figure 3 suggest that RIC-3 Ser-164 is a major target of TAX-6, mediating its effects on the acute (early) response to levamisole. Electrophysiological results of GABA application show that effects of TAX-6 seem to be mediated by altered GABA_A receptor activity (Figure 4C). If indeed RIC-3 Ser-164 is a target of TAX-6, its effects should also be mediated by altered GABA_A activity. To examine this possibility, we compared effects of *unc-49* (muscle-expressed GABA_A receptor subunit) knockdown on animals express-

ing minimal RIC-3 (control) or minimal RIC-3 S164E, which mimics phosphorylation. For these experiments, we used the muscle-expressed wild-type and S164E transgenes, as effects of the muscle-expressed S164E transgene are more robust (Figure 2, B compared to A) and, unlike the effects of RIC-3 S164E expressed from the *ric-3* promoter, are clearly seen in dsRNA-feeding experiments (Figure 5A compared to Figure 3, C and D). As expected, *unc-49* knockdown in transgenics expressing wild-type RIC-3 (control) leads to levamisole hypersensitivity (Vashlishan *et al.*, 2008; Figure 5A). However, in animals expressing the S164E mutant, *unc-49* knockdown had no significant effect compared with the same animals fed with control bacteria expressing an empty vector (Figure 5A). Moreover, levamisole responsiveness after *unc-49* knockdown in animals expressing wild-type RIC-3 was comparable to responsiveness of S164E animals fed with bacteria expressing empty vector (Figure 5A), consistent with effects of Ser-164 phosphorylation being mediated by reduced functional expression of UNC-49. We expect that loss of UNC-49 function will lead to higher sensitivity to levamisole relative to the RIC-3 S164E mutant; however, dsRNA feeding of *unc-49* reduces but does not eliminate UNC-49 function, as seen by its inability to produce the typical loss-of-function, shrinker, phenotype (McIntire *et al.*, 1993).

To further validate inhibitory effects of RIC-3 S164E on UNC-49 (GABA_A receptor), we used heterologous expression in *Xenopus laevis* oocytes. We previously showed that coexpressing RIC-3 mutants with nAChRs in *X. laevis* oocytes enables analysis of their mechanism of action (Cohen Ben-Ami *et al.*, 2005, 2009; Biala *et al.*, 2009). To examine effects of Ser-164 mutants on the body-wall muscle GABA_A receptor,

we coexpressed these mutants with the UNC-49B and UNC-49C subunits, which are known to assemble to form this receptor in vivo (Bamber *et al.*, 2003, 2005). Expression of the two UNC-49 subunits leads to robust GABA-dependent currents (Figure 5B). Coexpression of this receptor with the RIC-3 S164A mutant had no significant effect ($p = 0.08668$) on responses to GABA (Figure 5B), a result consistent with our previous results showing that RIC-3 is not needed for UNC-49 function in vivo (Halevi *et al.*, 2002). However, oocytes expressing the receptor with RIC-3 S164E showed significant reduction in GABA responses relative to oocytes expressing the receptor alone or with RIC-3 S164A (Figure 5B), results consistent with direct interaction of phosphorylated RIC-3 with this receptor, in contrast to an indirect effect via cell-specific mechanisms. Coexpression of wild-type RIC-3 had similar effects as coexpression with S164E and unlike effects of S164A (unpublished results), a result consistent with phosphorylation of this protein by casein kinase II, which is known to be strongly expressed in oocytes (Wilhelm *et al.*, 1995). Thus phosphorylation of RIC-3 at Ser-164 enables inhibition of GABA_A functional expression.

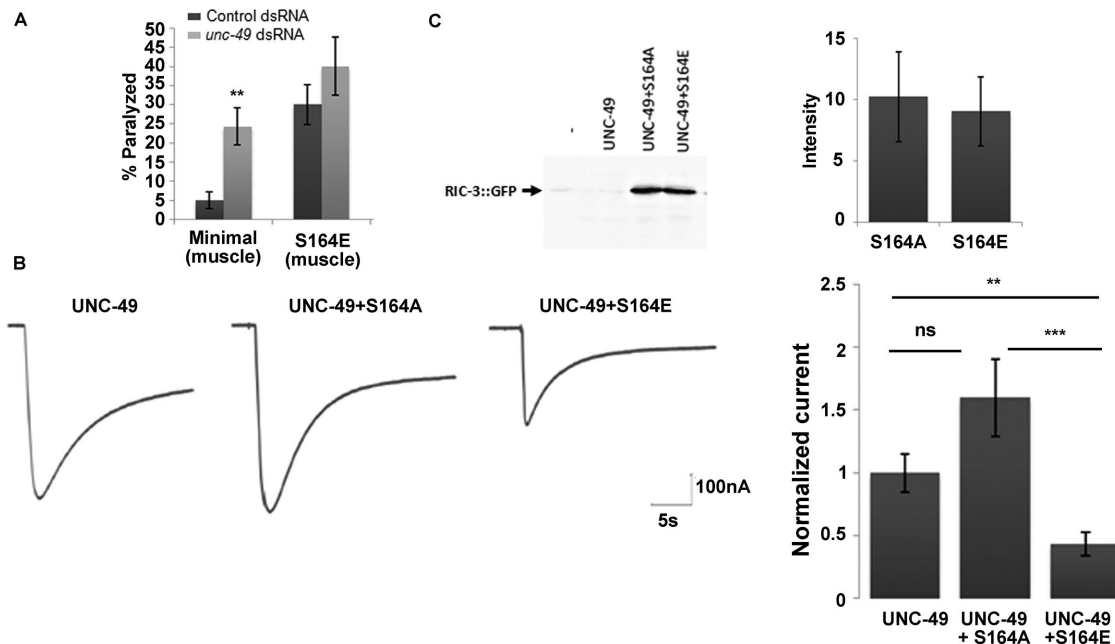


FIGURE 5: Effects of the S164E mutation are mediated by GABA_A inhibition. (A) Effects of *unc-49* knockdown are suppressed by the S164E mutation. Animals expressing minimal RIC-3 (Minimal) or minimal RIC-3 S164E (S164E) specifically in muscle in a wild-type background and treated with empty vector– (Control; dark gray) or *unc-49* dsRNA–expressing (light gray) bacteria. Percentage of animals paralyzed 60 min after being placed on levamisole. Significance is relative to the same strain fed with control dsRNA (empty vector) at the same time point; seven plates and $N = 3$ each. (B) Currents recorded from oocytes expressing UNC49 B/C alone (UNC-49), with RIC-3 minimal S164A (S164A), or with RIC-3 minimal S164E (S164E). Left, representative traces; right, average peak amplitudes normalized relative to average peak current amplitudes of receptor alone from the same experiment; $n = 26–31$ and $N = 3–4$. (C) Western analysis showing quantity of RIC-3 S164E and S164A mutants expressed in *X. laevis* oocytes with UNC-49 B/C. Left, representative Western analysis; right, average intensity (arbitrary units), three experiments. ** $p < 0.01$, *** $p < 0.001$.

To examine whether the reduced quantity of RIC-3 S164E (Figure 2C) is a result of intrinsic instability of this protein, we used Western analysis to compare quantities of S164E relative to S164A proteins in *X. laevis* oocytes injected with equal quantities of cRNAs encoding for the two proteins. This analysis shows no difference in the quantity of the two proteins (Figure 5C). Thus the reduced quantity of this protein in vivo and the reduced quantity of native RIC-3 after *tax-6* down-regulation (Figures 2C and 3B) are not due to intrinsic instability of the phosphorylation-mimicking mutant or of RIC-3 phosphorylated at Ser-164. Instead, this reduced quantity may depend on a muscle-specific factor recognizing RIC-3 S164E and Ser-164 phosphorylated RIC-3, a factor that, like BATH-42, directs its targets to degradation (Shteingauz *et al.*, 2009). Furthermore, results showing that, in spite of similar expression, S164E and S164A differently affect UNC-49 activity (Figure 5B) demonstrate that reduced RIC-3 quantity after phosphorylation of Ser-164 is not the cause of its inhibitory effects on UNC-49. Instead, phosphorylation of RIC-3 is likely to alter its conformation, enabling interaction with or inhibition of UNC-49.

KIN-10 functions opposite to TAX-6 to phosphorylate Ser-164

UNC-43, a calmodulin (CaM) kinase II homologue, functions opposite to TAX-6 in the regulation of levamisole sensitivity of vulval muscle (Lee *et al.*, 2004). Thus we examined whether it functions similarly in body-wall muscle. For this, we used *unc-43* dsRNA feeding in nonsensitized strains to focus on muscle-mediated functions of *unc-43*, as we did earlier for *tax-6* knockdown. *unc-43* knockdown, like *tax-6* knockdown, led to a significant increase in the sensitivity of body-wall muscles to levamisole within 30 min of exposure

(Figure 6A). Thus UNC-43 is unlikely to function opposite to TAX-6 in regulating body-wall muscle responsiveness to levamisole. Moreover, the RIC-3(S164A) mutation not only did not suppress effects of *unc-43* knockdown, instead it synergized with it, leading to a significant increase in sensitivity to levamisole, an increase not seen at this time point in S164A transgenics treated with control (empty vector) dsRNA or after *unc-43* knockdown in other *ric-3* transgenic strains (wild-type and S164E minimal RIC-3; Figure 6B). Thus UNC-43 is unlikely to target RIC-3 Ser-164.

Casein kinase II (KIN-10) was shown to function opposite to TAX-6 in *C. elegans* cilia (Hu *et al.*, 2006). Furthermore, bioinformatics (scansite.mit.edu and www.phosida.com; Supplemental Table S2) suggests several casein kinase II targets within RIC-3, including Ser-164. To examine whether KIN-10 is likely to function opposite to TAX-6 in body-wall muscle, we examined its effects on levamisole-dependent paralysis. *kin-10* knockdown significantly reduces the effects of levamisole on body-wall muscles (Figure 6C), a result consistent with KIN-10 functioning opposite to TAX-6. To examine whether KIN-10 targets RIC-3 Ser-164, we examined whether mutations in this site reduce the effects of KIN-10 knockdown. Indeed, S164A reverses (15 min) and later (30 min) eliminates (Figure 6, D and E) effects of *kin-10* dsRNA on levamisole responsiveness of body-wall muscle. Elimination of the effects of *kin-10* dsRNA is also observed in the S164E mutant (Figure 6, D and E). Thus our results are consistent with KIN-10 phosphorylating and TAX-6 dephosphorylating RIC-3 at Ser-164 to regulate levamisole responsiveness of body-wall muscle. Reversal of the effects *kin-10* knockdown in S164A mutants (Figure 6D) can be explained by the unmasking of other KIN-10 targets having opposite effects on levamisole responsiveness. Finally,

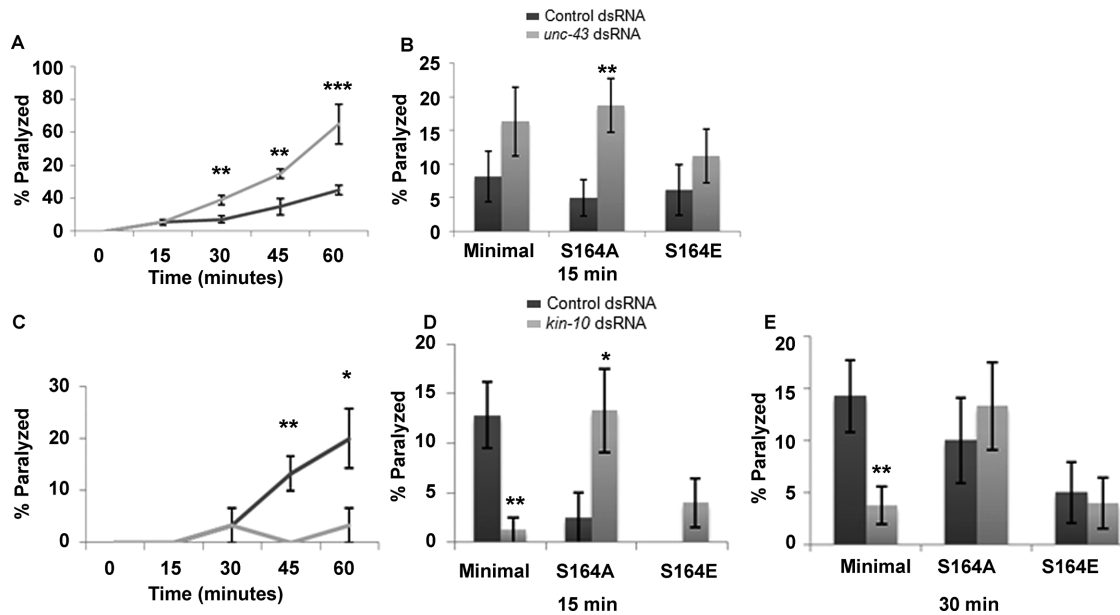


FIGURE 6: KIN-10, but not UNC-43, functions opposite to TAX-6. (A) Levamisole sensitivity of wild-type animals fed with empty vector– (Control; dark gray) or *unc-43* dsRNA–expressing (light gray) bacteria. Percentage of animals paralyzed at different time points after being placed on plates containing levamisole (0.2 mM). Significance is relative to animals fed with control dsRNA at the same time point; 11 plates and four independent experiments. (B) Effects of *unc-43* knockdown are not suppressed by Ser-164 mutations. Animals expressing minimal RIC-3 (Minimal), minimal RIC-3 S164A (S164A), or minimal RIC-3 S164E (S164E) in a *ric-3(md1181)* background and fed with empty vector– (Control; dark gray) or *unc-43* dsRNA–expressing (light gray) bacteria. Percentage of animals paralyzed 15 min after being placed on levamisole. Significance is relative to the same strain fed with control dsRNA (empty vector) at the same time point; 8–11 plates, $N = 4$ each. (C) Levamisole sensitivity of wild-type animals fed with empty vector– (Control; dark gray) or *kin-10* dsRNA–expressing (light gray) bacteria. Percentage of animals paralyzed at different time points after being placed on plates containing levamisole (0.2 mM). Significance is relative to animals fed with control dsRNA at the same time point; three plates and $N = 2$. (D, E) Effects of *kin-10* knockdown are suppressed by Ser-164 mutations. Animals expressing minimal RIC-3 (Minimal), minimal RIC-3 S164A (S164A), or minimal RIC-3 S164E (S164E) in a *ric-3(md1181)* background and treated with empty vector– (Control; dark gray) or *kin-10* dsRNA–expressing (light gray) bacteria. Percentage of animals paralyzed 15 (D) or 30 (E) min after being placed on levamisole. Significance is relative to the same strain fed with control dsRNA (empty vector) at the same time point; four to eight plates and $N = 3$ each. * $p < 0.05$, ** $p < 0.01$, *** $p < 0.001$.

we note that whereas TAX-6 down-regulation reduces RIC-3 quantity in body-wall muscle (Figure 3B), KIN-10 down-regulation does not affect RIC-3 quantity in these muscles (unpublished results).

DISCUSSION

RIC-3 was previously shown to be a nAChR-specific chaperone (Halevi *et al.*, 2002). Results described here show that phosphorylation of RIC-3 Ser-164 enables inhibitory effects of RIC-3 on GABA_A receptors. Thus our work identified a new target for this evolutionarily conserved chaperone. Such promiscuous interactions are consistent with previous work suggesting that RIC-3 is a disordered protein (Cohen Ben-Ami *et al.*, 2009); intrinsically disordered proteins have flexible interaction surfaces, enabling interactions with divergent targets. Moreover, phosphorylation of such proteins strongly affects their specificity and their effects, even switching from positive to negative effects, as reviewed in Tompa *et al.* (2005).

C. elegans body-wall muscles are an experimentally tractable and well-characterized model for analysis of signaling pathways regulating E-I balance. Here we show that phosphorylation of RIC-3, known to promote maturation of nAChRs mediating excitatory input to muscle, enables inhibition of GABA_A receptors mediating the inhibitory input to muscle. RIC-3 Ser-164 phosphorylation is unlikely to interfere with the positive effects of this protein on L-AChR,

mediating excitatory inputs to muscle. Instead, it enables interaction with and inhibition of an additional target. Thus RIC-3 phosphorylation enables coordinated regulation of excitation and inhibition, providing a novel mechanism for fine-tuning E-I balance.

Our results are consistent with phosphorylated RIC-3 Ser-164 inhibiting functional expression of GABA_A receptors in *C. elegans* body-wall muscle. RIC-3 Ser-164 was shown to be phosphorylated in *C. elegans* by Zielinska *et al.* (2009). Thus loss-of-function mutations in RIC-3 should lead to higher responses to GABA due to release of body-wall muscle GABA_A receptors from inhibition. However, our previous analysis showed no such effect (Halevi *et al.*, 2002). This apparent contradiction can be resolved if, under normal growth conditions, phosphorylation levels of RIC-3 Ser-164 in body-wall muscles are low. This explanation does not contradict findings of the phosphoproteomic analysis, as RIC-3 is expressed widely (Halevi *et al.*, 2002), and tissue distribution of phosphorylated sites identified in this study is unknown (Zielinska *et al.*, 2009). Moreover, body-wall muscle excitability of RIC-3 S164A transgenics is similar to excitability of transgenics expressing wild-type RIC-3, a result consistent with our suggestion that under normal growth conditions, TAX-6–dependent dephosphorylation of RIC-3 Ser-164 in body-wall muscle is efficient, leading to low-level RIC-3 Ser-164 phosphorylation and no inhibition by RIC-3 of GABA_A receptors in body-wall muscle.

We note, however, that effects of KIN-10 knockdown on muscle excitability appear to contradict this suggestion. This contradiction is resolved by bioinformatics (Supplemental Table S2) and deletion analysis of RIC-3 (unpublished results), suggesting residues in the C-terminus of RIC-3 as major KIN-10 targets mediating much of its effects on muscle excitability—residues that are missing in the minimal RIC-3 fragment used in this study.

Knockdown of both calcineurin (TAX-6) and CaM kinase II (UNC-43) increase muscle excitability. Our work shows that knockdown of calcineurin affects excitability via decreased inhibition. Similarly, it was shown that CaM kinase II loss of function reduced muscle GABA_A receptor synaptic abundance and function (Liu *et al.*, 2007; Vashlishan *et al.*, 2008). Our results showing a synergistic effect of RIC-3 S164A and CaM kinase II knockdown are consistent with interactions between two parallel pathways affecting the same target. This, together with previous work from several labs, suggests a complex network of signaling pathways regulating E-I balance in the *C. elegans* neuromuscular junction—pathways affecting both neurotransmitter release and postsynaptic receptors (Liu *et al.*, 2007; Vashlishan *et al.*, 2008; Jospin *et al.*, 2009; Stawicki *et al.*, 2013).

Calcineurin activity depends on both calmodulin and calcium, thus serving as a sensor for synaptic activity (Baumgärtel and Mansuy, 2012). TAX-6, the *C. elegans* calcineurin A homologue, was previously shown to physically interact with the muscle nAChR, L-AChR (Gottschalk *et al.*, 2005). Work presented here shows no effect of TAX-6 knockdown or loss of function on L-AChR abundance or function. The increased levamisole sensitivity observed in TAX-6–knockdown animals (Figure 3A) is thus an indirect consequence of reduced GABA_A receptor activity, as *tax-6(lf)* caused no increase in levamisole-induced currents, yet decreased GABA currents (Figure 4, B and C). In the light of these findings, earlier results showing increased nicotine sensitivity in *tax-6(lf)* mutants (Gottschalk *et al.*, 2005) are likely due to effects on the GABA_A receptor. We therefore propose that instead of regulating L-AChR function, TAX-6 serves as a sensor for its activity as part of a homeostatic mechanism. Specifically, increased muscle excitation via the highly calcium permeable L-AChR (Boulin *et al.*, 2008) should activate TAX-6, leading to dephosphorylation of its targets such as RIC-3, thus releasing inhibitory GABA_A receptor from suppression by phosphorylated RIC-3 and leading to a homeostatic decrease in muscle excitability.

MATERIALS AND METHODS

Strains and plasmids

Minimal RIC-3 is a minimal functional fragment containing the conserved RIC-3 domain (two transmembrane domains followed by a coiled-coil domain) but lacking the nonconserved N'-terminus, the C'-terminus domain, which includes a second coiled-coil domain, and the alternatively retained exon (Figure 1). The transgene containing this fragment and the surrounding 5' and 3' *ric-3* genomic sequences has been described (Biala *et al.*, 2009). RIC-3 S164 present in this fragment was mutated to glutamate to obtain the S164E construct and to alanine to obtain the S164A construct. The mutated fragments were obtained by overlapping PCR using primers *glu1-gcgaagaagagaaattttgatgaggaag* and *glu2-catcatcatcgtcttctcatcaaaataattt* for S164E and *ala1-gcgaagaagagaaattttgatgaggaag* and *ala2-catcatcatcgtcttctcatcaaaataattt* for S164A.

The full-length RIC-3 (wild type), minimal RIC-3, S164E, and S164A constructs were tagged with GFP downstream to the first coiled-coil domain (RIC-3 wild type) and at the end of the RIC-3 fragment (minimal RIC-3, S164A, and S164E) and placed under the *myo-3* promoter or the *ric-3* promoter. These constructs were injected at 5 ng/μl together with *rol-6* DNA (pRF4) as marker at

50 ng/μl. This DNA mix was supplemented with SKII–DNA at 80 ng/μl. Transgenes expressed from the *ric-3* promoter were injected into *ric-3(md1181)* animals, whereas transgenes expressed from the *myo-3* promoter were injected into wild-type (N2) animals.

Wild-type (N2 Bristol) and all other strains were grown on nematode growth medium (NGM) plates seeded with OP50 at 20°C (Wood, 1988)

dsRNA feeding experiments

Plasmids and bacteria for dsRNA feeding–mediated knockdown were obtained from the Ahringer library (Kamath *et al.*, 2003). Induction of dsRNA expression was done in liquid broth (LB) plus ampicillin using 4 mM isopropyl-β-D-thiogalactoside (IPTG) for 3 h. The bacteria (HT115DE3) expressing the desired vector dsRNA were then spun down, resuspended using M9 buffer (0.02 M KH₂PO₄, 0.042 M Na₂HPO₄, 0.085 M NaCl, and 1 mM MgSO₄) plus 5 mM IPTG and seeded on NGM plates. For dsRNA-feeding experiments, L4 animals were transferred to plates seeded with dsRNA-expressing bacteria and grown for one generation at 20°C. Then L4 animals from these plates were transferred to fresh plates with new dsRNA-expressing bacteria 20–22 h before paralysis assays. As a control, the same strain was grown on bacteria-expressing empty vector.

Levamisole assays

For paralysis assays, L4 animals were picked 20–22 h before each experiment for growth on fresh plates at 20°C. Levamisole assays were done on 10 young adult animals per NGM plate containing 0.2 mM levamisole. At each time point after placing the animals on the levamisole-containing plate (time zero), each animal was examined for its response to gentle prodding; animals not moving in response to prodding were considered paralyzed.

Experiments were done at room temperature (18–25°C). Because room temperature affects the kinetics of the response to levamisole, we cannot compare response kinetics between experiments, and therefore each experiment includes a control strain.

Imaging and immunohistochemistry

Rabbit polyclonal antibodies were generated by injection of the C-terminus of RIC-3 fused to glutathione S-transferase, and the resulting serum was affinity purified on Affigel 15 (Shteingauz *et al.*, 2009). Immunohistochemistry was done after picric acid fixation as previously described (Yassin *et al.*, 2001), using a 1:1000 dilution of the anti-RIC-3 antibody and a 1:300 dilution of Alexa Fluor 488 anti-rabbit antibodies. Before staining, RIC-3 antibodies were incubated overnight with *ric-3(md1181)* animals to remove nonspecific antibodies. RIC-3 was observed and quantified at body-wall muscle and neurons in *tax-6* (*p675*); *lin15(n765ts)* animals expressing the transgene [jEx92 [*pmyo-3::tax-6* cDNA g.o.f.; *lin-15+*] relative to muscle of *tax-6* (*p675*); *lin15(n765ts)*, which lost the transgene and were identified by having multiple vulva (Gottschalk *et al.*, 2005). Fluorescence intensity in muscle is relative to neurons, as they are weakly affected by dsRNA (Sieburth *et al.*, 2005) or do not express the *tax-6(gf)* transgene. Similarity between results obtained in the two experiments—one normalizing to wild-type neurons and the other normalizing to *tax-6(lf)* neurons—are consistent with TAX-6 having no effect on RIC-3 quantity in neurons.

Images and quantification of *unc-63::yfp* (Boulin *et al.*, 2012) and of *ric-3::gfp* fluorescence were obtained after mounting in a 5-μl drop of M9 with 25 mM sodium azide placed on an agar pad (2% agar). Worms were transferred to this drop, and after they were paralyzed, a coverslip was placed on top and sealed with 50%/50%

Paraplast/paraffin. To reduce variability due to different imaging conditions, intensity was normalized relative to the average intensity measured in the same day of one of the strains examined.

For imaging, animals were synchronized by eye as L4 or young adults. Images were taken using a Zeiss (Germany) LSM710 confocal microscope using a Plan-Apochromat 63×/1.40 differential interference contrast oil objective (Figures 2–4) or Plan-NeoFluar 40×/1.30 objective (Supplemental Figure S1) and a 488-nm (Figures 2 and 3 and Supplemental Figure S1) or 514-nm laser (Figure 4). For quantification of GFP fluorescence, we avoided saturation by adjusting the gain on the strain showing higher expression before image acquisition using the systems software, and all images for a specific experiment were taken using the same parameters. These images were analyzed by summing the total fluorescence in a manually defined region of interest, using ZEN 2012 software. To examine altered distribution due to RIC-3 aggregation, we used the coefficient of variation, which is the SD of fluorescence intensity in the region of interest divided by the mean fluorescence intensity in the same region (Shteingauz *et al.*, 2009).

Electrophysiology in *C. elegans*

For electrophysiology experiments, *tax-6(p675)* was outcrossed twice. Electrophysiology of *C. elegans* body-wall muscles was done as previously described (Richmond and Jorgensen, 1999; Nagel *et al.*, 2005). Animals were immobilized with Histoacryl glue (B. Braun Surgical, Spain), and a lateral incision was made to access neuromuscular junctions along the ventral nerve cord. The basement membrane overlying the muscles was enzymatically removed by incubation in 0.5 mg/ml collagenase for 10 s (type IV, C5138; Sigma-Aldrich, Germany). Muscle cells were patch clamped in a whole-cell voltage-clamp mode at room temperature (20–22°C) at a holding potential of –60 mV using an EPC10 amplifier with head stage connected to a standard HEKA (Lambrecht/Pfalz, Germany) pipette holder for glass capillaries (outer diameter, 1.0 mm) using fire-polished borosilicate pipettes (1B100F-4; outer diameter, 1.0 mm; World Precision Instruments, Berlin, Germany) of 4- to 7-M Ω resistance. The bath solution contained NaCl, 150 mM; KCl, 5 mM; CaCl₂, 5 mM; MgCl₂, 1 mM; glucose, 10 mM; sucrose, 5 mM; and 4-(2-hydroxyethyl)-1-piperazineethanesulfonic acid (HEPES), 15 mM, pH 7.3; with NaOH, ~330 mOsm. The pipette solution contained KCl, 120 mM; KOH, 20 mM; MgCl₂, 4 mM; *N*-Tris[hydroxymethyl]methyl-2-aminoethane-sulfonic acid, 5 mM; CaCl₂, 0.25 mM; sucrose, 36 mM; ethylene glycol tetraacetic acid, 5 mM; and Na₂ATP, 4 mM, pH 7.2; with KOH, ~315 mOsm. Using these solutions at holding potential –60 mV and as previously described (Richmond and Jorgensen, 1999), the chloride gradient in the body wall muscle cells is reversed, and GABA currents therefore appear as inward currents due to chloride efflux through GABA receptor channels. GABA or levamisole (100 μ M) was pressure-applied (Picospritzer III; Parker Hannifin, Contamine-sur-Arve, France) onto dissected muscle cells, and corresponding inward currents were measured in whole-cell mode. Data were analyzed by Patchmaster software (HEKA Electronics, Germany).

Heterologous expression and electrophysiology in *Xenopus* oocytes

UNC-49B and C constructs for oocytes expression were a kind gift from Bruce Bamber (University of Toledo, Toledo, OH) (Bamber *et al.*, 2003). RIC-3 (S164A and S164E) for oocyte expression were generated by mutating the previously described RIC-3 minimal-expressing plasmid using the primers described; these plasmids have a GFP marker downstream and in-frame to RIC-3 (Cohen Ben-Ami *et al.*, 2005). For in vitro transcription, plasmids were linearized with

Asp718 I (UNC-49B and C) NheI(ric-3 minimal-WT; and S164E) or NotI(S164A), and cRNA was transcribed using T3 RNA polymerase (Ambion, France) for UNC-49B and C or T7 RNA polymerase (Promega, Fitchburg, WI) for RIC-3 constructs. In vitro synthesis and injection of cRNAs into oocytes was previously described (Cohen Ben-Ami *et al.*, 2005). Briefly, in vitro-transcribed and capped cRNAs were injected at final concentrations of 0.25 ng/oocyte for *unc-49B* and C and 5 ng for GFP-tagged *ric-3* S164A or S164E. At 2–3 d after injections, cells were placed in a 2-ml bath that was perfused with medium and penetrated with two 0.5- to 1.5-M Ω 3 M KCl-filled glass microelectrodes attached to a GeneClamp 500B amplifier (Axon Instruments, Foster City, CA) using a two-electrode voltage clamp with active ground configuration and an HS-2A head stage (Axon Instruments). A Pentium 4 PC system employing the pCLAMP9 (AxoScope) software (Axon Instruments) was used for maintaining voltage clamp. Cells were clamped at –70 mV. Oocytes with leak currents <250 nA were used.

Electrodes were filled with 3 M KCl. The extracellular recording solution contained ND96 (96 mM NaCl, 2 mM KCl, 5 mM MgCl₂, 5 mM HEPES, pH 7.5). The current and the voltage in the voltage-clamp circuit were recorded simultaneously and saved directly onto the computer. The 1 mM GABA agonist (Sigma-Aldrich) was prepared and used to stimulate oocytes. Results are presented as mean \pm SEM, with *n* the number of oocytes tested and *N* the number of different frogs in each experiment.

Western analysis

For Western analysis, oocytes were homogenized by repetitive pipetting in 25 μ l/oocyte buffer (20 mM Tris-HCl, pH 8.0, 100 mM NaCl, 1% Triton X-100) with Complete Mini, EDTA-free, protease inhibitor mixture tablets (Roche Applied Science, Switzerland; 1 tablet/7 ml of buffer). After 30 min on ice, the homogenate was centrifuged at 4°C. The supernatant was aliquoted, and sample buffer (4 \times Laemmli sample buffer [Bio-Rad, Hercules, CA] + 10% β -mercaptoethanol + 90 mM dithiothreitol) was added at 1:2 buffer-to-sample ratio.

Proteins were separated on 10% SDS-PAGE, transferred to polyvinylidene fluoride membrane and immunoblotted with 1:1000 rabbit anti-GFP antibody (MBL, Woburn, MA) followed by 1:5000 goat-anti rabbit secondary antibody (Jackson laboratories, New Market, UK). Band intensity was quantified by ImageJ software (Schneider *et al.*, 2012).

Statistical analysis

In all experiments, *n* is number of animals, plates (for levamisole assays), or oocytes examined and *N* is the number of independent experiments or frogs. Results are given as average \pm SEM. Significance was examined using two-sided Student's *t* tests.

ACKNOWLEDGMENTS

We thank Jean-Louis Bessereau for the UNC-63::YFP strain, Bruce Bamber for *unc-49B* and C clones, and the *Caenorhabditis* Genetics Center (St. Paul, MN) for strains. This work was funded by Israel Science Foundation Grants 352/10 and 388/15 and Deutsche Forschungsgemeinschaft Grant EXC115 (Cluster of Excellence Frankfurt).

REFERENCES

- Bamber BA, Richmond JE, Otto JF, Jorgensen EM (2005). The composition of the GABA receptor at the *Caenorhabditis elegans* neuromuscular junction. *Br J Pharmacol* 144, 502–509.
- Bamber BA, Twyman RE, Jorgensen EM (2003). Pharmacological characterization of the homomeric and heteromeric UNC-49 GABA receptors in *C. elegans*. *Br J Pharmacol* 138, 883–893.

- Baumgärtel K, Mansuy IM (2012). Neural functions of calcineurin in synaptic plasticity and memory. *Learn Mem* 19, 375–384.
- Biala Y, Liewald JF, Cohen Ben-Ami H, Gottschalk A, Treinin M (2009). The conserved RIC-3 coiled-Coil domain mediates receptor-specific interactions with nicotinic acetylcholine receptors. *Mol Biol Cell* 20, 1419–1427.
- Boulin T, Gielen M, Richmond JE, Williams DC, Paoletti P, Bessereau JL (2008). Eight genes are required for functional reconstitution of the *Caenorhabditis elegans* levamisole-sensitive acetylcholine receptor. *Proc Natl Acad Sci USA* 105, 18590–18595.
- Boulin T, Rapti G, Briseño-Roa L, Stigloher C, Richmond JE, Paoletti P, Bessereau JL (2012). Positive modulation of a Cys-loop acetylcholine receptor by an auxiliary transmembrane subunit. *Nat Neurosci* 15, 1374–1381.
- Cheng A, McDonald NA, Connolly CN (2005). Cell surface expression of 5-hydroxytryptamine type 3 receptors is promoted by RIC-3. *J Biol Chem* 280, 22502–22507.
- Cohen Ben-Ami H, Biala Y, Farah H, Elishevit E, Battat E, Treinin M (2009). Receptor and subunit specific interactions of RIC-3 with nicotinic acetylcholine receptors. *Biochemistry* 48, 12329–12336.
- Cohen Ben-Ami H, Yassin L, Farah H, Michaeli A, Eshel M, Treinin M (2005). RIC-3 affects properties and quantity of nicotinic acetylcholine receptors via a mechanism that does not require the coiled-coil domains. *J Biol Chem* 280, 28053–28060.
- Eichler SA, Meier JC (2008). E-I balance and human diseases—from molecules to networking. *Front Mol Neurosci* 1, 2.
- Gottschalk A, Almedom RB, Schedletzky T, Anderson SD, Yates JR, Schafer WR (2005). Identification and characterization of novel nicotinic receptor-associated proteins in *Caenorhabditis elegans*. *EMBO J* 24, 2566–2578.
- Halevi S, McKay J, Palfreyman M, Yassin L, Eshel M, Jorgensen E, Treinin M (2002). The *C. elegans ric-3* gene is required for maturation of nicotinic acetylcholine receptors. *EMBO J* 21, 1012–1020.
- Halevi S, Yassin L, Eshel M, Sala F, Sala S, Criado M, Treinin M (2003). Conservation within the RIC-3 gene family: effectors of nAChR expression. *J Biol Chem* 278, 34411–34417.
- Hu J, Bae YK, Knobel KM, Barr MM (2006). Casein kinase II and calcineurin modulate TRPP function and ciliary localization. *Mol Biol Cell* 17, 2200–2211.
- Jospin M, Qi YB, Stawicki TM, Boulin T, Schuske KR, Horvitz HR, Bessereau JL, Jorgensen EM, Jin Y (2009). A neuronal acetylcholine receptor regulates the balance of muscle excitation and inhibition in *Caenorhabditis elegans*. *PLoS Biol* 7, e1000265.
- Kamath RS, Fraser AG, Dong Y, Poulin G, Durbin R, Gotta M, Kanapin A, Bot NL, Moreno S, Sohrmann M, et al. (2003). Systematic functional analysis of the *Caenorhabditis elegans* genome using RNAi. *Nature* 421, 231–237.
- Lansdell SJ, Gee VJ, Harkness PC, Doward AI, Baker ER, Gibb AJ, Millar NS (2005). RIC-3 enhances functional expression of multiple nicotinic acetylcholine receptor subtypes in mammalian cells. *Mol Pharmacol* 68, 1431–1438.
- Lee J, Jee C, Song HO, Bandyopadhyay J, Lee JI, Yu JR, Park BJ, Ahnn J (2004). Opposing functions of calcineurin and CaMKII regulate G-protein signaling in egg-laying behavior of *C.elegans*. *J Mol Biol* 344, 585–595.
- Lei M, Xu H, Li Z, Wang Z, O'Malley TT, Zhang D, Walsh DM, Xu P, Selkoe DJ, Li S (2016). Soluble A β oligomers impair hippocampal LTP by disrupting glutamatergic/GABAergic balance. *Neurobiol Dis* 85, 111–121.
- Lewis JA, Wu CH, Berg H, Levine JH (1980a). The genetics of levamisole resistance in the nematode *Caenorhabditis elegans*. *Genetics* 95, 905–928.
- Lewis JA, Wu CH, Levine JH, Berg H (1980b). Levamisole-resistant mutants of the nematode *Caenorhabditis elegans* appear to lack pharmacological acetylcholine receptors. *Neuroscience* 5, 967–989.
- Liu Q, Chen B, Ge Q, Wang ZW (2007). Presynaptic Ca²⁺/calmodulin-dependent protein kinase II modulates neurotransmitter release by activating BK channels at *Caenorhabditis elegans* neuromuscular junction. *J Neurosci* 27, 10404–10413.
- Martin RJ, Robertson AP, Buxton SK, Beech RN, Charvet CL, Neveu C (2012). Levamisole receptors: a second awakening. *Trends Parasitol* 28, 289–296.
- McIntire SL, Jorgensen E, Horvitz HR (1993). Genes required for GABA function in *Caenorhabditis elegans*. *Nature* 364, 334–337.
- Nagel G, Brauner M, Liewald JF, Adeishvili N, Bamberg E, Gottschalk A (2005). Light activation of channelrhodopsin-2 in excitable cells of *Caenorhabditis elegans* triggers rapid behavioral responses. *Curr Biol* 15, 2279–2284.
- Petrash HA, Philbrook A, Haburcak M, Barbagallo B, Francis MM (2013). ACR-12 ionotropic acetylcholine receptor complexes regulate inhibitory motor neuron activity in *Caenorhabditis elegans*. *J Neurosci* 33, 5524–5532.
- Richmond JE, Jorgensen EM (1999). One GABA and two acetylcholine receptors function at the *C. elegans* neuromuscular junction. *Nat Neurosci* 2, 791–797.
- Schneider CA, Rasband WS, Eliceiri KW (2012). NIH Image to ImageJ: 25 years of image analysis. *Nat Methods* 9, 671–675.
- Shteingauz A, Cohen E, Biala Y, Treinin M (2009). The BTB-MATH protein BATH-42 interacts with RIC-3 to regulate maturation of nicotinic acetylcholine receptors. *J Cell Sci* 122, 807–812.
- Sieburth D, Ch'ng Q, Dybbs M, Tavazoie M, Kennedy S, Wang D, Dupuy D, Rual JF, Hill DE (2005). Systematic analysis of genes required for synapse structure and function. *Nature* 436, 510–517.
- Stawicki TM, Takayanagi-Kiya S, Zhou K, Jin Y (2013). Neuropeptides function in a homeostatic manner to modulate excitation-inhibition imbalance in *C. elegans*. *PLoS Genet* 9, e1003472.
- Tomba P, Szász C, Buday L (2005). Structural disorder throws new light on moonlighting. *Trends Biochem Sci* 30, 484–489.
- Vashlishan AB, Madison JM, Dybbs M, Bai J, Sieburth D, Ch'ng Q, Tavazoie M, Kaplan JM (2008). An RNAi screen identifies genes that regulate GABA synapses. *Neuron* 58, 346–361.
- Wilhelm V, Rojas P, Gatica M, Allende CC, Allende JE (1995). Expression of the subunits of protein kinase CK2 during oogenesis in *Xenopus laevis*. *Eur J Biochem* 232, 671–676.
- Wood WB (1988). *The Nematode Caenorhabditis elegans*. Cold Spring Harbor, NY: Cold Spring Harbor Laboratory.
- Yassin L, Gillo B, Kahan T, Halevi S, Eshel M, Treinin M (2001). Characterization of the DEG-3/DES-2 receptor: a nicotinic acetylcholine receptor that mutates to cause neuronal degeneration. *Mol Cell Neurosci* 17, 589–599.
- Zielinska DF, Gnäd F, Jedrusik-Bode M, Wisniewski JR, Mann M (2009). *Caenorhabditis elegans* has a phosphoproteome atypical for metazoans that is enriched in developmental and sex determination proteins. *J Proteome Res* 8, 4039–4049.